Methods for efficient computation and visualization of magnetic flux lines in 3D

Martin Hafner[1], Marc Schöning[1], Marcin Antczak[2], Andrzej Demenko[2] and Kay Hameyer[1]
1 - Institute of Electrical Machines – RWTH Aachen University
2 - Institute of Electrical Engineering and Electronics – Poznan University of Technology
E-mail: Martin.Hafner@IEM.RWTH-Aachen.de, Marcin.Antczak@doctorate.put.poznan.pl

***Abstract*—Flow visualization is essential to provide an insight into complex flow patterns of electromagnetic devices. In this paper, a method for the detection and evenly-spaced seeding of closed flux lines in 3D quasi-static electromagnetic fields is presented. The seeding is performed by weighting the magnetic flux on a specified cutting surface. Due to discretization of a finite element simulation, which is also applied for the flux density solution, the force lines are usually not closed. Therefore, an algorithm is introduced, monitoring the force line computation, to provide the generation of closed force lines.**

I. Introduction

An intuitive method for the visualization of vector fields are flux lines, which provide a straightforward visual impression of the field characteristic and the magnetic circuit. Applying this technique to an electromagnetic field solution, one directly encounters the problem of closed flux line computation arising from its solenoidal field characteristics. In this paper, a method is introduced that monitors the stream computation to detect closed curves and minimize the computational effort. Afterwards, the flux line algorithm is combined with a seeding strategy that places starting points in correlation with the flux on a specified cutting surface to support quick flow pattern recognition. The proposed method is generally applicable to the electromagnetic field and comparable flow fields such as eddy current distributions.

II. Closed Flux Line Computation

A. Flux Line Computation

A flux line is an oriented curve ρ in a vector field ν on a domain Ω, which is everywhere tangential to the vector flow, with the properties

$$\frac{\partial \rho}{\partial \tau}\left(\tau\right) = \nu\left(\rho\left(\tau\right)\right) \tag{1}$$

$$\rho\left(\tau = 0\right) = a \tag{2}$$

where $\rho\left(\tau\right)$ is a certain point on the flux line, $\nu\left(\rho\left(\tau\right)\right)$ the corresponding field vector and a an arbitrary start point in Ω. Each point in Ω is strictly mapped to exact one curve ρ.

According to Maxwell equations, the evoked electromagnetic vector field has an solenoidal field characteristic, so that each flux line ρ has a characteristic, but unknown length L, where

$$\rho\left(\tau + n\cdot L\right) = \rho\left(\tau\right), \forall n \in \mathbb{N} \ . \tag{3}$$

For a given start point $\rho\left(\tau = 0\right)$, the flux line ρ is obtained by integrating (2) iteratively over a discrete length $\Delta\tau$ (integration step length), yielding

$$\rho\left(\tau + \Delta\tau\right) = \rho\left(\tau\right) + \int_{\tau}^{\tau+\Delta\tau} \nu\left(\rho\left(\tau\right)\right)\partial\tau \tag{4}$$

For a rapid and accurate flux line computation, (4) is solved by using a fourth-order Runge-Kutta integrator with adaptive step size and error control [1].

B. Closed Loop Detection

In general, the numeric solution of (4) leads to a continuous summation of the integration error, so that a computed curve does not comply to (3), a typical example is given in fig. 1. To detect such closed flux lines, without any knowledge of

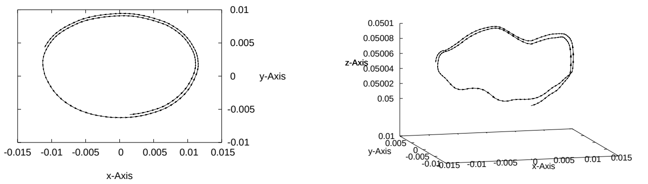

(a) Spiral progress of flux line in x-y plane.

(b) Displacement fluctuation, $\leq 1\%$, in z-direction.

Fig. 1. Typically integration error of eq. (4) in 3D Space. Top and lateral view of a flux line around a current excited rectangular wire in z direction.

the location and shape within the magnetic field, stop criteria are necessary that evaluate the integration process step-by-step and detect the characteristic length L. Basically, an end point $\rho\left(\tau_i\right)$ is located in a sphere around $\rho\left(\tau_0\right)$ with an error radius ϵ, e.g.

$$\left\|\rho\left(\tau_i\right) - \rho\left(\tau_0\right)\right\| \leq \epsilon \ . \tag{5}$$

Since the mesh size of Ω typically varies, e.g. in the comparison of an air gap to a back yoke, a more accurate end point detection is required.

Therefore the basic idea of the algorithm is to monitor the integration process and evaluate a modification of (5) by only verifying a possible closing of the curve in 3D space. Counting the number of sign reversal in:

$$\delta\left(\tau_{i+1}\right) = \left\|\rho\left(\tau_{i+1}\right) - \rho\left(\tau_i\right)\right\| \cdot \left\|\rho\left(\tau_1\right) - \rho\left(\tau_0\right)\right\| \tag{6}$$

A closed curve, independent from the simulated geometry, requires at least $2k+1, k \in \mathbb{N}^0$ sign alternations. For point candidates that meet the latter precondition, the point distance perpendicular to the stream direction, given by

$$\left\|\left(\rho\left(\tau_i\right) - \rho\left(\tau_0\right)\right) \times \left(\rho\left(\tau_1\right) - \rho\left(\tau_0\right)\right)\right\| \leq \epsilon \tag{7}$$

is computed and compared to ϵ. The error control by (7) is, in contrast to (5), independent from the displacement in curve direction, caused by the variable step size $\Delta\tau$.

III. Seeding Strategy

Magnetic flux lines provide a visual impression of the vectorial field direction, and if colorized an additional information of the intensity of magnetic field density. To support a quick recognition of the flow pattern by a set of flux lines, their seeding points have to be correlated with the magnitude of the vector field. By this requirement, the better part of seed points is located in an area with high field values and vice versa. Therefore, in this paper a seed point computation on a user defined cutting surface, $C \subseteq \Omega$, is presented. The proposed algorithm is as follows:

- Initially, the flux on all cutting elements in C is evaluated by

$$\Phi = \vec{B}_C \cdot \vec{a}_C \tag{8}$$

  where $\vec{B}_C$ is the vectorial flux per element and $\vec{a}_C$ the corresponding oriented surface vector.
- According to a used specified flux range $[\Phi_{min}, \Phi_{max}]$, the plane C is sub-divided into a given number N_{plane} of sub-planes

$$C = \{C_1, C2, \cdots, C_{N_{plane}}\} \tag{9}$$

  so that each sub-domain contains all elements with the corresponding flux interval.
- To weight the flux in each sub-domain C_i, the average flux $\Phi_i^{average}$ over all elements N_{C_i} on C_i, given by

$$\Phi_i^{average} = \sum_i^{N_{C_i}} \Phi_i^{elem} \tag{10}$$

  is computed, [2], [3].
- For a given number of starting point N_{tot}, the ratio of

$$N_i = \frac{\Phi_i^{average}}{\sum_i^{N_{plane}} \Phi_i^{average}} N_{tot} \tag{11}$$

  defines the number of seeding point per sub-domain N_i.

In the final step of the seeding algorithm, the points N_i are placed in the sub-domains C_i. At present state, the starting points are moved to those elements within C_i which have the largest magnitude of the magnetic flux. This leads, as exemplified in fig. 3, to a rough evenly-spaced seeding. An alternative placing strategy is to place N_i on the inner boundary of C_i equidistantly. The latter method is in preparation and will be discussed and compared to the flux-value-based seeding strategy in the full paper.

IV. Application

A rectangular wire surrounded by air is used as a test model for the seeding strategy in combination with the presented closed flux line algorithm presented in section II-B and III. The source current density J_s is injected into the cross section area of the wire. Fig 2, visualized by [4], shows the applied test scenario together with its vectorial representation of the flux density distribution, obtained by [5]. Fig. 3 shows the seed point distribution of 100 start point, by a chosen flux interval from 50 to 100 and a decomposition into 10 subdomains. It can be noticed, that the starting point population density increases by a distance reduction from the wire. The latter provides a visual impression of the flux density distribution. The flux lines are rough evenly-space which helps to recognize the corresponding flow pattern.

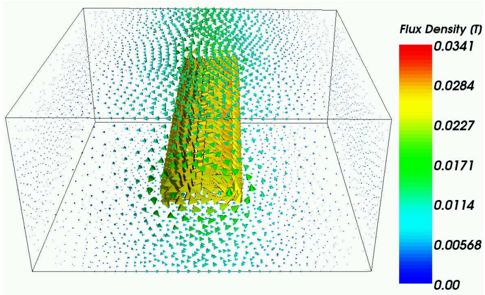

Fig. 2. Current excited rectangular wire in z direction together with its flux density distribution.

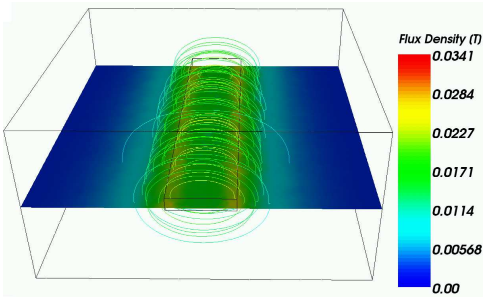

Fig. 3. Closed flux lines seeded around the current excited rectangular wire.

V. Conclusion

In this paper, an algorithm which detects closed flux lines by extending the integration process by a monitoring routine is presented. The method relies on the assumption of a solenoidal vector field characteristic. To give a visual impression of the vector field solution, a seeding strategy is presented which places seeding points in correlation with the magnetic flux on a cutting surface. As a first test case, the proposed method is exemplified on a 3D air surrounded wire model yielding a flux line distribution which corresponds to the expected flow field pattern.

References

[1] J. D. Lambert, *Numerical Methods for Ordinary Differential Systems: The Initial Value Problem*. Wiley, Sep. 1991.

[2] V. Cingoski, T. Kuribayashi, K. Kaneda, and H. Yamashita, "Improved interactive visualization of magnetic flux lines in 3-D space using edge finite elements," *Magnetics, IEEE Transactions on*, vol. 32, no. 3, pp. 1477–1480, 1996.

[3] X. Ye, D. Kao, and A. Pang, "Strategy for seeding 3D streamlines," in *Visualization, 2005. VIS 05. IEEE*, 2005, pp. 471–478.

[4] I. Kitware, *VTK User's Guide Version 5*, 5th ed. Kitware, Inc., Sep. 2006.

[5] D. van Riesen, C. Monzel, C. Kaehler, C. Schlensok, and G. Henneberger, "iMOOSE-an open-source environment for finite-element calculations," *Magnetics, IEEE Transactions on*, vol. 40, no. 2, pp. 1390–1393, 2004.